

# Adaptive Predictive Controller for a Servo Drive – Actuator/Sensor Failure Study Experiments

Dariusz Horla

*Institute of Control and Information Engineering, Faculty of Electrical Engineering, Poznan University of Technology,  
ul. Piotrowo 3a, 60-965, Poznan, Poland*

**Keywords:** Predictive Control, Actuator Failure, Sensor Failure, Robust System.

**Abstract:** The paper considers the problem of predictive control with actuator or sensor failures. The problem is to show in what configuration (i.e. for what prediction horizons) the adaptive generalized predictive control can tolerate these failures, assuring similar performance in comparison with the case without failures. The results are shown on the basis of experiments conducted on the laboratory stand with a servo drive coupled with a mechanical backlash module to mimic actuator/sensor failures, and with a magnetic brake, to show the performance in the case of occurrence of an unexpected load.

## 1 INTRODUCTION

In order to obtain knowledge concerning a model of a plant, adaptive control (enabling automatic tuning of controller parameters) can be used to improve control performance, using recursive identification algorithms to obtain estimates in an on-line fashion.

Receding horizon strategy in controls and predictive control are relatively new methods in industrial process control, in which a repeated optimization is performed at every sampling instant. Since optimization procedures are usually iterative-based, then even in the case of the Generalised Predictive Controller (GPC) a computational load must be taken into account when implementing this control method in real-time regime.

In the paper, the GPC controller implemented as C-MEX S-function (Horla, 2016) is used to control the Modular Servo System of Inteco, using a USB interface and LAPACK library to perform necessary matrix computations in the case of actuator/sensor failures, to verify the applicability of the GPC method (or its robustness) against unmodelled work regimes, such as imprecise measurements or unexpected changes in control signal. In addition, the case of brake failure, what mimics constant and unexpected load on the shaft, is also taken into consideration.

It is of practical importance to know if the control system can tolerate any failures in its components. The design-based approaches are to design the controller in such a way, as to enhance its capability

of being robust against failures or uncertainty, as in (Yang et al., 2000b; Yang et al., 2000a; Zuo et al., 2010). On the other hand, in the paper (Mhaskar et al., 2006) the authors do take predictive control into consideration, but to build a bank of controllers with special switching law in the case of an identified failure. In this paper, it is the control system that has been analyzed from the viewpoint of possible failures and their impact on the control performance, resulting with the information concerning applicability of the GPC method in such situations, and extending the results presented in (Horla, 2016).

The experimental setup is a servo drive with the FPGA-based controller, allowing hardware-in-the-loop experiments, and enabling rapid prototyping of control algorithms to evaluate their performance. The experimental setup is described on the basis of (Horla, 2013) and (Horla, 2016).

Section 2 shortly describes the experimental setup, Section 3 gives model description and equations of the GPC controller, taken from (Horla, 2016). Section 4 presents the results of the experiments, and the last Section summarizes the whole paper.

## 2 EXPERIMENTAL SETUP

The Inteco's experimental setup comprises the DC motor (12 V, 77 W, 250 mNm, speed 3000 rpm, current 4.7 A), tachogenerator and inertia load (brass cylinder, 2 kg, diameter 66 mm, length 68 mm), as shown in Figure 1 (Inteco, a), (Inteco, b). The DC

motor drives the inertia load and tachogenerator that is connected directly to the DC motor, with voltage proportional to the angular velocity, and  $y(t) = \dot{\theta}(t)$  as its output. Additional modules of the laboratory setup include encoder or magnetic brake modules.

The command input is fed to the servo drive from an input-output card used by Real-Time Workshop (MathWorks, 2015) and Simulink in order to work in real-time regime. C-mex S-functions have been used to implement the controller algorithm and estimation scheme that has been downloaded to the FPGA board. The control armature voltage  $e_a(t)$  is limited to  $\pm 12$  V, and is presented in the paper in dimensionless form as  $|u(t)| \leq 1$ .

The considered servo has the nonlinear static characteristic related to the presence of a friction torque, which has been compensated by its inverse, leading to linear system equations (when no saturation occurs in dynamic states) (Horla, 2013; Horla, 2016).

In accordance with (Horla, 2016), assuming the following formula for the armature loop  $i_a(t)$ :

$$e_a(t) = R_a i_a(t) + L \frac{di_a(t)}{dt} + e_m(t),$$

constant flux and

$$e_m(t) = k_e \dot{\theta}(t)$$

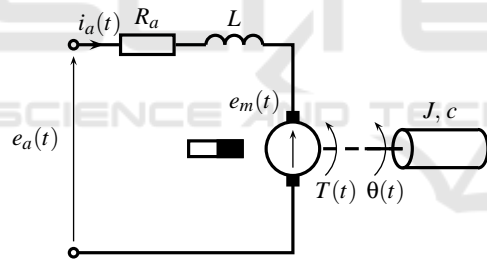


Figure 1: Diagram of experimental setup (Horla, 2013).

with the electromechanical torque  $T(t) = k_T i_a(t)$ , one gets

$$T(t) = J\ddot{\theta}(t) + c\dot{\theta}(t).$$

Now, neglecting armature inductance, the „true” continuous-time model transfer function becomes

$$G(s) = \frac{k_T}{R_a J s + R_a c + k_e k_T} = \frac{k}{1 + sT}$$

with:

$$k = \frac{k_T}{R_a c + k_e k_T}, \quad T = \frac{R_a J}{R_a c + k_e k_T}.$$

It is assumed that the ZOH-discretized model of this plant is taken into consideration when implementing the GPC algorithm with the sampling period of  $T_S = 0.1$  s.

### 3 PLANT MODEL

After linearization and assuming there is a noise corrupting measurements, the model takes the form:

$$A(q^{-1})y_t = B(q^{-1})u_{t-d} + C(q^{-1})\xi_t,$$

where  $u_t$  and  $y_t$  are input and output signals, respectively,  $\xi_t$  is assumed to be a white noise with zero mean value and  $d$  is a dead time. The introduced polynomials are given as:

$$\begin{aligned} A(q^{-1}) &= 1 + a_1 q^{-1} + a_2 q^{-2} + \dots + a_{nA} q^{-nA}, \\ B(q^{-1}) &= b_0 + b_1 q^{-1} + b_2 q^{-2} + \dots + b_{nB} q^{-nB}, \\ C(q^{-1}) &= 1 + c_1 q^{-1} + c_2 q^{-2} + \dots + c_{nC} q^{-nC}. \end{aligned}$$

Since the GPC control enables tracking of a reference signal  $r_t$  known  $N_y$  samples in advance (Camacho and Bordons, 1998), (Maciejowski, 2001), the controller computes  $N_u$  consecutive control signals, to minimize the performance index given as

$$J = \sum_{i=d}^{N_y} (r_{t+i} - \hat{y}_{t+i})^2 + q_u \sum_{i=1}^{N_u} (\Delta v_{t+i-1})^2, \quad (1)$$

where:

$\hat{y}_{t+i}$  is an optimal  $i$ -step output prediction,  $q_u$  is a control signal weight,  $N_u$  and  $N_y$  are control and prediction horizons, respectively.

By solving the following Diophantine equations (Camacho and Bordons, 1998):

$$\Delta A(q^{-1})E_i(q^{-1}) + q^{-i}F_i(q^{-1}) = C(q^{-1}), \quad (2)$$

$$C(q^{-1})G_i(q^{-1}) + q^{-i}\Gamma_i(q^{-1}) = E_i(q^{-1})B(q^{-1}), \quad (3)$$

where  $i$  denotes output prediction step, the following polynomials are obtained ( $n\Gamma = \max(nB - 1, nC - 1)$ ):

$$\begin{aligned} E(q^{-1}) &= 1 + e_1 q^{-1} + \dots + e_{i-1} q^{-i+1}, \\ F(q^{-1}) &= f_0 + f_1 a^{-1} + \dots + f_{nA} q^{-nA}, \\ \Gamma(q^{-1}) &= \gamma_0 + \gamma_1 q^{-1} + \dots + \gamma_{n\Gamma} q^{-n\Gamma}, \\ G(q^{-1}) &= g_0 + g_1 q^{-1} + \dots + g_{i-1} q^{-i+1}. \end{aligned}$$

The polynomials introduced above enable one to compute  $N_y$  step output prediction as a sum of forced and free responses:

$$\hat{y}_{t+1} = G\Delta v_t + \underline{f}_{t+1}, \quad (4)$$

where:

$\hat{y}_{t+1} = [\hat{y}_{t+1}, \dots, \hat{y}_{t+N_y}]^T$  is the prediction of the

output,

$G$  is an impulse response matrix, i.e. with entries from  $G_i(q^{-1})$ ,

$\Delta \underline{v}_t = [\Delta v_t, \dots, \Delta v_{t+N_u-1}]^T$  is a computed control signal vector,

$\underline{f}_{t+1} = [\hat{y}_{t+1/t}, \dots, \hat{y}_{t+N_y/t}]^T$  is a free response vector.

In the unbounded case, and for (1), an explicit formula for the control signal might be obtained:

$$\begin{cases} \Delta \underline{u}_t = \Delta \underline{v}_t = (G^T G + q_u I)^{-1} G^T (\underline{r}_{t+1} - \underline{f}_{t+1}) \\ \underline{u}_t = \Delta \underline{u}_t + \underline{u}_{t-1} \end{cases} \quad (5)$$

When constraints become active  $u_t \neq v_t$ , and control signal  $u_t$  applied to the plant has a different amplitude than the computed control signal  $v_t$ .

Since the Inteco Servo drive can be modeled as the first-order inertia  $G(s) = \frac{k}{1+sT}$  in velocity control task, its discrete-time model is given with  $nA = 1$ ,  $nB = 0$ ,  $d = 1$ , i.e.:

$$A(q^{-1}) = 1 - aq^{-1}, \quad B(q^{-1}) = b.$$

From the solution of the Diophantine equations with the assumed model, a sample form of prediction (4) can be presented 3 steps ahead (a general rule can be observed on this prediction):

$$\begin{bmatrix} \hat{y}_{t+1} \\ \hat{y}_{t+2} \\ \hat{y}_{t+3} \end{bmatrix} = \begin{bmatrix} b & 0 & 0 \\ (a+1)b & b & 0 \\ (a^2+a+1)b & (a+1)b & b \end{bmatrix} \begin{bmatrix} \Delta v_t \\ \Delta v_{t+1} \\ \Delta v_{t+2} \end{bmatrix} + \begin{bmatrix} (a+1)y_t - ay_{t-1} \\ (a^2+a+1)y_t - a(a+1)y_{t-1} \\ (a^3+a^2+a+1)y_t - a(a^2+a+1)y_{t-1} \end{bmatrix}$$

that enables an easy way of generation of control signals according to (5). In addition,  $\Gamma_i(q^{-1}) = \gamma_0 = 0$ ,  $G_i(q^{-1}) = bE_i(q^{-1})$ , and it is assumed that  $C(q^{-1}) = 1$ .

The details of implementation in C code are given in (Horla, 2016). The next section presents experimental results obtained from the laboratory stand with sampling period  $T_S = 0.1$  s.

## 4 ACTUATOR/SENSOR FAILURE CONSIDERATIONS

### 4.1 Preliminaries

All the to-be-presented experimental results have been carried out in a fully adaptive system using the

on-line RLS identification scheme of the model of the plant in the closed-loop system, with the initial estimates equal to half of their true values (identified in a long time horizon for sufficiently exciting input signal) and forgetting factor equal to unity (Åström and Wittenmark, 1989). The results are connected with classical IAE and ISE performance indices calculated on the basis of continuous-time signals from the tracking system, being standard integrals of absolute or squared tracking errors in the whole experiment horizon (formulas omitted for the sake of brevity). Every measurement set has been carried out as a set of 55 experiments (all possible  $N_u \leq N_y$  configurations), repeated 4 times, with mean values presented.

The following cases are taken into consideration, when considering robustness of the GPC control scheme of this plant to unmodelled situations:

- velocity sensor failure (mechanical backlash module between brass cylinder and encoder),
- actuator failure (mechanical backlash module between DC motor and brass cylinder),
- brake failure (magnetic brake module included in the system).

All the performance indices are presented as differences between the case with the selected failure model, and the nominal case with no failure (for selected configuration of prediction horizons), both in the sense of absolute value change and relative (i.e. percentage) change – positive values refer to performance deterioration, and negative – improvement.

### 4.2 Sensor Failure Results

As has been already remarked, the mechanical backlash unit has been connected in series between the DC motor with brass cylinder module and the encoder, to model sensor failure. In this way, any change in information in dynamic states is generated by the encoder when a full rotation of the shaft is made for the velocity control task. With such a configuration of the system, four series of measurements have been carried out, in analogy to the series presented in (Horla, 2016).

As can be seen from Figure 2, the worst performance deterioration takes place whenever  $N_u$  and  $N_y$  take on small values simultaneously, and the situation improves with increasing  $N_y$ . Performance indices for  $N_y = 10$  are superior. In the case of percentage change consideration, the intermediate performance deterioration for larger  $N_y$  results from small values of the indices considered in experiments without failure. In Figure 2(e), the results of a sample experiment have

been presented for the situation with and without actuator failure with the same configuration of the controller.

The considered sensor failure model results in poorer tracking during transients, but is of no meaning in steady-state, i.e. for the stages with constant reference signal. In the adaptive system, it results in oscillatory behaviour of the closed-loop system, improving performance of the identification algorithm.

It turns out that when failure of this kind takes place, the best strategy is to keep a relatively long  $N_y$  and short  $N_u$ , this way the control action is mostly abrupt, allowing faster transients. In the case of longer  $N_u$  horizon, the expected change in control signal extends over a number of samples, deteriorating the performance during reverse of the shaft.

### 4.3 Actuator Failure Results

After connecting the mechanical backlash between the DC motor and the brass cylinder, the system with actuator failure model has been obtained. In this configuration, the greatest absolute increase of performance indices is observed for  $N_u = N_y = 1$ , i.e. in one-step predictive controller. The situation improves with increasing  $N_y$ . To the great surprise, for  $N_u = 1$  and  $N_y = 10$  the both performance indices improved in comparison with failure-free situation.

As can be seen from Figure 3, the considered actuator failure had no impact again on the steady-state performance, but on increasing the dominating time constant of the closed-loop system. The system was slower, since it was impossible to change the velocity of the shaft fast enough during reverse working mode, due to the backlash.

Similar conclusions apply here as in the case of the considered model of the sensor failure – the shaft rotates faster leading to transfer the generated torque sooner, as in the case of low-velocity rotation.

### 4.4 Brake Failure

In order to conduct this part of experiments, the laboratory setup hitherto considered had to be modified, and between the magnetic brake has been included the brass cylinder and the encoder. During rotation, due to Faraday's law of induction, the current is induced which magnetic fields generate load torque, according to Lenz's law. In this part, only two measuring series have been performed each composed of 55 simple measurements (see Fig. 4).

As expected, this situation must be connected with overall performance degradation, which is, however, neglectful for small  $N_u$  and large  $N_y$  configuration. It

is inadvisable to choose both large horizons of control and prediction, since the identified model is inaccurate (it does not take the load into account).

By observing the tracking performance presented in Figure 4(e), it can be said that brake failure (i.e. introduction of braking past some failure) results in changes with control signal, but it does not alter closed-loop system dynamics excessively.

Surprisingly, in the case of unexpected automatic brake failure, already twice-mentioned configuration of prediction horizons, enables one to improve the control performance, by getting slower transients and in this way, filtering-out of possible oscillations in the error signal.

## 5 SUMMARY

The paper analyzed the situation of failures of the control system and their impact on predictive controller behaviour in such cases, to obtain a reliable control system. It was interesting to verify if the GPC scheme can tolerate any failures either in actuator or sensor, thus this analysis was basically of practical interest, enforced by presenting the results from a real laboratory stand. In the future, it would be interesting to verify if the sampling period allow one to obtain any better improvement or reliability of the control system.

## ACKNOWLEDGEMENTS

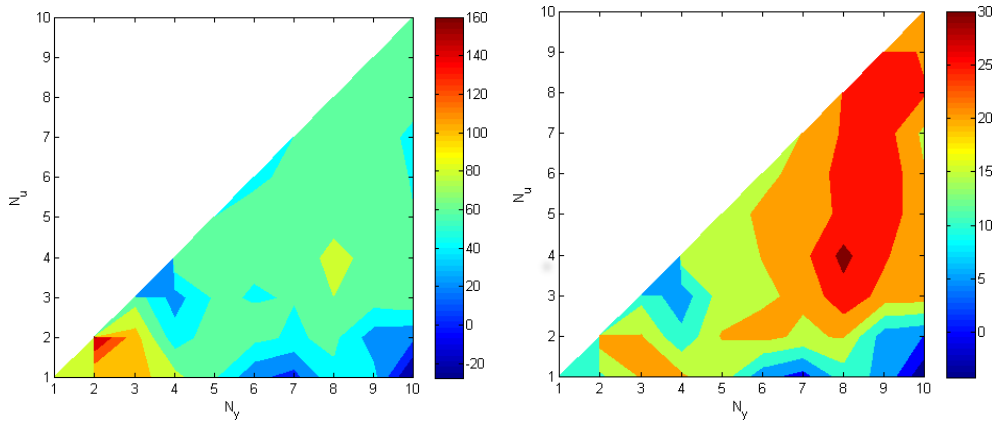
The author wishes to thank to Mr. Pawel Szczygiel for his help with performing necessary measurements.

## REFERENCES

- Åström, K. and Wittenmark, B. (1989). *Adaptive Control*. Addison-Wesley.
- Camacho, E. and Bordons, C. (1998)., *Model Predictive Control*, pages 51–83. Springer.
- Horla, D. (2013). Minimum variance adaptive control of a servo drive with unknown structure and parameters. *Asian Journal of Control*, DOI:10.1002/asjc.479, 15(1):120–131.
- Horla, D. (2016). C-code implementation of an adaptive real-time GPC velocity controller for a servo drive. In *Proceedings of the 17th International Conference on Mechatronics*, pages 1–6.
- Inteco. *Modular Servo System USB version Installation Manual*. Inteco.
- Inteco. *Modular Servo System User's Manual*. Inteco.

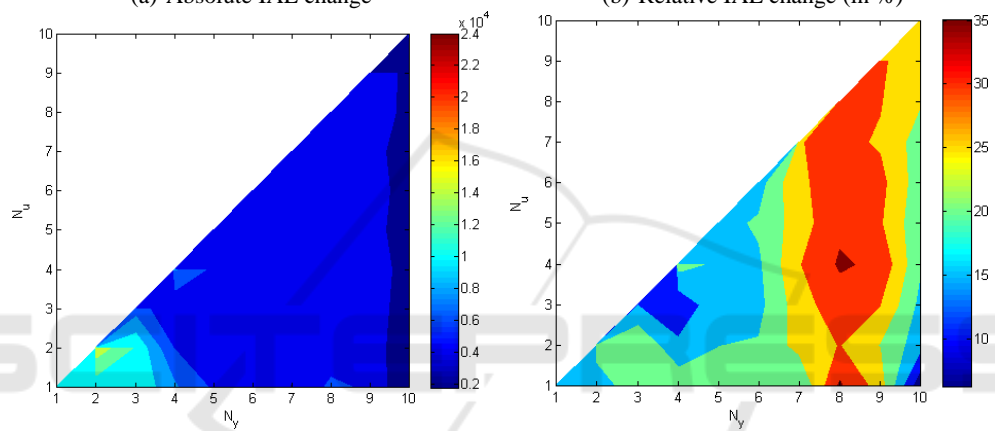
- Maciejowski, J. (2001). *Predictive Control with Constraints*. Pearson, UK.
- MathWorks (2015). *Real-time Workshop User's Manual*. MathWorks.
- Mhaskar, P., Gani, A., and Christofides, P. (2006). Fault-tolerant control of nonlinear processes: Performance-based reconfiguration and robustness. In *American Control Conference*.
- Yang, G.-H., Wang, J., and Soh, Y. (2000a). Reliable lqg control with sensor failures. *IEE Proceedings – Control Theory and Applications*, 147(4):433–439.
- Yang, Y., Yang, G.-H., and Soh, Y. (2000b). Reliable control of discrete-time systems with actuator failures. *IEE Proceedings – Control Theory and Applications*, 147(4):428–432.
- Zuo, Z., Ho, D., and Wang, Y. (2010). Fault tolerant control for singular systems with actuator saturation and nonlinear perturbation. *Automatica*, 46:569–576.





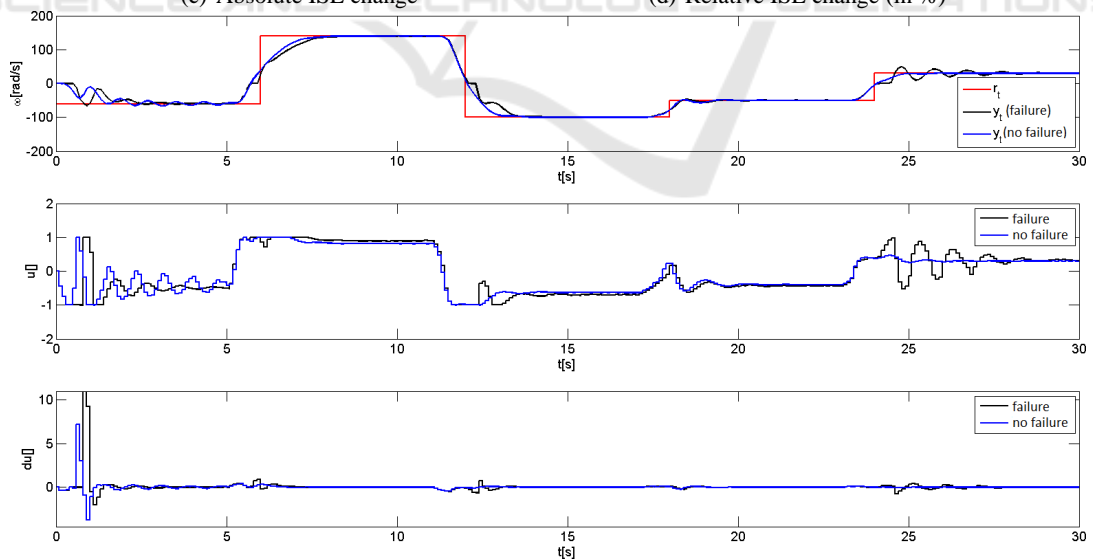
(a) Absolute IAE change

(b) Relative IAE change (in %)



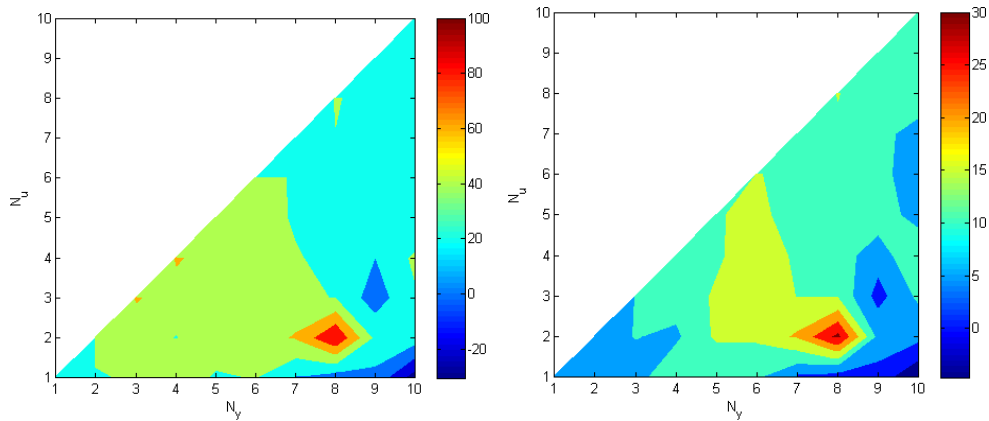
(c) Absolute ISE change

(d) Relative ISE change (in %)



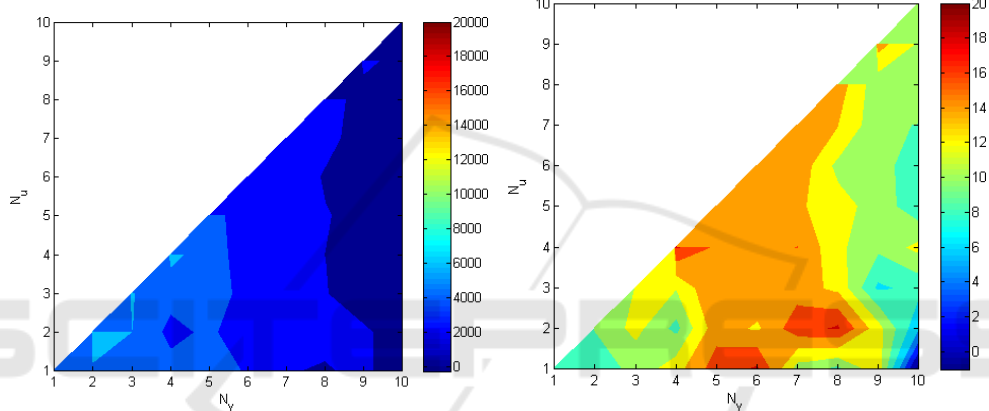
(e) Tracking performance with and without sensor failure,  $N_u = 5$ ,  $N_y = 10$

Figure 2: Experimental results concerning sensor failure with  $q_u = 16,000$ ,  $T_S = 0.1$  s.



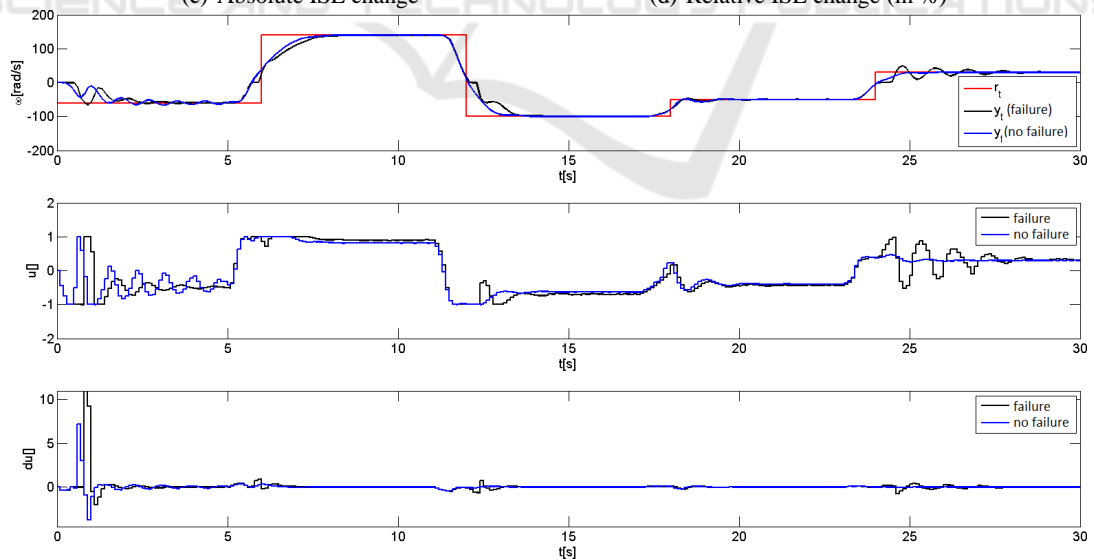
(a) Absolute IAE change

(b) Relative IAE change (in %)



(c) Absolute ISE change

(d) Relative ISE change (in %)



(e) Tracking performance with and without actuator failure,  $N_u = 5$ ,  $N_y = 10$

Figure 3: Experimental results concerning actuator failure with  $q_u = 16,000$ ,  $T_S = 0.1$  s.

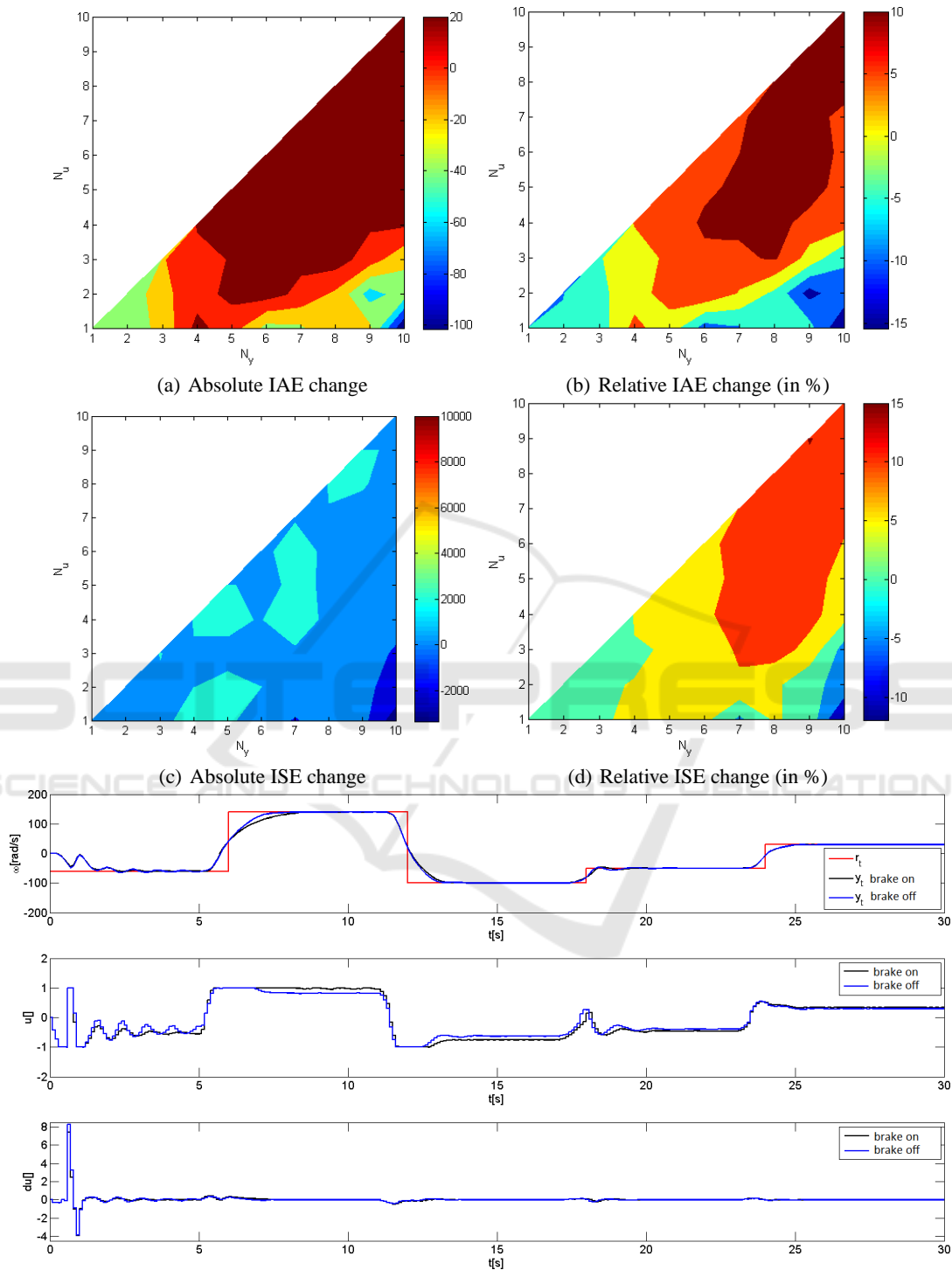


Figure 4: Experimental results concerning brake failure with  $q_u = 16,000, T_S = 0.1$  s.